ANALYSIS OF LOW FREQUENCY VARIABILITY PATTERNS AND CIRCULATION REGIMES OVER SOUTHERN SOUTH AMERICA AND THEIR RESPONSE TO GLOBAL WARMING AS DEPICTED BY IPCC AR4 AOGCMS

Silvina A. Solman [*] and Natalia Pessacg
CIMA-CONICET/UBA – Dto. Cs. de la Atmósfera y los Océanos (UBA)- Buenos Aires, Argentina

1. INTRODUCTION

Most of the studies on the climate change issue have focused on discerning trends and persistent changes forced by anthropogenic increases of greenhouse gases. Nevertheless, in recent years the changes in variability have drawn special attention. Moreover, there has been a considerable effort in understanding whether the recent observed climate variations are induced by anthropogenic forcing or are part of the natural variability of our climate system (Marshall, 2003). Important issues include how modes of variability will change under anthropogenic forcing and whether the response of the climate system will project onto modes of internal variability. Recent studies have shown the importance and relevance of analysing the climate change signal as a projection onto pre-existing natural modes of internal variability of the atmosphere (Stone et al., 2001; Hsu and Zwiers, 2001). An immediately associated question is to know whether climate change also affects the modes on which it projects. Palmer (1999) suggested that the climate response to an external forcing might cause a change in the occurrence frequency of recurrent flow patterns associated with natural variability, rather than a change in the modes themselves. Several studies focused on the Northern Hemisphere have confirmed this approach and shown the relevance of modifications in the temporal statistics of recurrent regimes of atmospheric states to describe climate change (Solman and Le Treut, 2006; Hsu and Zwiers 2001, Kageyama et al. 1999).

Leading modes of low-frequency extratropical variability in the SH can be characterised basically by two dominant modes: a high-latitude vacillation, which modulates the strength of the polar vortex, the so-called Antarctic Oscillation (AAO), and a Rossby wave train propagating over the South Pacific towards southern South America and then refracting equatorward into the Atlantic, referred to as the Pacific-South America mode (PSA). These dominant modes are often identified in terms of the first few empirical orthogonal functions (EOFs) of analysed geopotential height data, at 500 hPa, 700 hPa or at 850 hPa (Mo and Higgins, 1998). They arise as the main modes of variability from interannual to interdecadal time-scales, being the AAO the dominant mode when interannual variability is retained in the analysis. PSA-like mode arises as a dominant mode of variability at low frequencies from intraseasonal to interannual and interdecadal time-scales as well. It is important to remark that the behaviour and characteristics of the main modes of variability are geographically-

dependent (Yang and Reinhold 1991) and thus, results from a sectorial analysis may differ from hemispheric ones.

In a recent study focused on the response of the low-frequency variability to increased greenhouse gas concentration in a sector comprising southern South America and surrounding oceans, Solman and Le Treut (2006) analyzed the behaviour of low-frequency variability patterns of the atmospheric circulation from a transient simulation performed with the IPSL CCM2 coupled global model, in which the greenhouse forcing is continuously increasing. They found that the main modes of low-frequency variability remain stationary throughout the simulation, suggesting they depend more on the internal dynamics of the atmospheric flow than on its external forcing. Inspection of the circulation regimes that represent the more recurrent patterns at interannual and interdecadal time-scales showed that climate change manifests itself as a change in regime population, suggesting that the negative phase of the Antarctic Oscillation -like pattern becomes more frequented in a climate change scenario. Changes of regime occurrence were superimposed to a positive trend whose spatial pattern is reminiscent of the structure of the Antarctic Oscillation -mode of variability. The change in regime frequencies of the circulation patterns of low-frequency variability were found to be in opposite phase with respect to the trend, thus, the behaviour of these patterns of variability, superimposed to a changing mean state, modulates the climate change signal. Carril et al. (2005), Fyfe et al. (1999) and Kushner et al. (2000), focusing mainly in the behaviour of the AAO-mode confirm that the climate change signal in the mid to higher latitudes of the Southern Hemisphere projects strongly onto the positive phase of the AAO.

In this study we analyze several last generation 20th and 21st century simulations performed with a set of 8 Atmosphere - Ocean General Circulation Models (AOGCMs) participating in the IPCC Fourth Assessment Report (AR4). The availability of this set of experiments represents an invaluable opportunity to address several questions about the future behavior of the climate system in the state-of-art of the main tool to investigate future scenarios of climate change. The focuses of this study are twofold. First, to evaluate the capability of the AOGCMs in representing the observed (as depicted by NCEP reanalysis) main leading modes of low-frequency variability, ranging from interannual to interdecadal time-scales, and trends. Second, to evaluate the response of the main modes of variability to anthropogenic forcing, as depicted by the 21st century simulations under the A2 emission

[*] Corresponding author address: Ciudad Universitaria Pabellón II- 2° piso (1428) Buenos Aires- Argentina
Tel: 54 11 4787 2693 email: solman@cima.fcen.uba.ar

scenario. Climate change is being analyzed in terms of changes in the frequency of occurrence and/or changes in the spatial characteristics of recurrent flow patterns associated with natural variability at interannual and intradecadal time-scales. We also explore the spatial pattern of the climate change signal (the linear trend) in order to evaluate the contribution of both, the trend and the internal variability response.

2. DATA AND METHODS

We have analyzed outputs from 8 AOGCMs: 1) UKMO-HadCM3 (Hadley Centre for Climate Prediction and Research / Met Office, UK); 2) MPI-ECHAM5/MPI-OM (Max Planck Institute for Meteorology, Germany); 3) GFDL-CM2.0 (NOAA, Geophysical Fluids Dynamics Laboratory, USA); 4) IPSL-CM4 (Institut Pierre Simon Lapace, France); 5) NCAR-CCSM3 (National Center for Atmospheric Research, USA); 6) MIROC3.2 (Center for Climate System Research, Japan / National Institute for Environmental Studies, Japan / Frontier Research Center for Global Change, Japan); 7) CSIRO-Mk3.0 (CSIRO Atmospheric Research, Australia) and 8) CNRM-CM3 (Centre National de Recherches Meteorologiques, Meteo-France, France). Documentation of these models is available on the PCMDI web site (http://www-pcmdi.llnl.gov). Model outputs from the climate of the 20th Century experiment (20C3M) from 1950 to 2000 and from the SRES A2 experiment, from year 2000 up to year 2099 were processed. Only one realization of each simulation has been used for the analysis. The focus of our study is to evaluate the behavior of the low-frequency variability patterns, thus, all calculations are based on monthly mean 500 hPa heights. Anomalies are defined with respect to a 11-year running mean throughout the period 1950-2099. The observed reference which is used to evaluate the performance of the models in terms of patterns of low-frequency variability is the NCEP reanalysis data for the period 1950-2000.

The domain chosen extends from 160°W to 0° and from 80°S to 20°S, in order to capture the patterns that affect southern South American climate.

We adopt the same methodology described in Solman and LeTreut (2006). The main modes of low-frequency variability are defined as the leading EOFs calculated as the covariance matrix. EOF analysis is used to check the consistency of model results with observed data, and also as a manner to check the stability of the simulations in terms of pattern configuration. Then, we performed a cluster analysis, based on the algorithm described in Michelangeli et al. (1995), which constitutes the most convenient way to diagnose the population of different climate regimes and describe their evolution throughout time. The cluster analysis is performed in a reduced EOF space (represented by the first 8 EOFs). Assuming a predetermined number of clusters the algorithm starts from a set of as many random seeds as the chosen number of clusters and finds a partition of the entire dataset

that minimizes the sum of variances within each cluster. In order to find the optimal number of clusters the clustering algorithm is run 50 times from different initial sets of random seeds and a classifiability index is calculated as the average of pattern correlation among the members of each partition. The higher the classifiability index, the more similar the members of each partition are and, then, the more robust the classification is. In order to set significance limits for this index this is compared to the results from a first order Markov process having the same covariance matrices at lags 0 and 1 as the initial data set. The classifiability index is then calculated for 100 random samples and the upper and lower bound of confidence are assigned to the 10th highest and 10th lowest values of these indices. Then, the classifiability index of the true data set is compared with these bounds and the optimal number of clusters is defined as the one in which the classifiability index of the true data set is higher than that of the red noise model (MVL). The algorithm determines the more recurrent patterns and the more statistically significant partition.

3.   RESULTS

Figure 1 shows the first three EOFs as depicted by NCEP reanalysis dataset and the simulated twentieth century climate by the 8 AOGCMs. It is important to remark that this analysis is not focused in searching for one best model, but it tends to evaluate the capability of the state-of-art AOGCMs in reproducing the characteristics of the observed large-scale low-frequency variability patterns and to analyze its response under anthropogenic forcing.

Overall, all models are capable of capturing adequately the ranking and the spatial structure of the leading EOFs from a sectorial approach. The first EOF, referred to as the AAO-mode, is characterized by a zonally symmetric structure with anomalies of opposite sign over sub-polar regions and mid-latitudes, presenting a wave-number 3 structure. This mode is well represented, though almost all models tend to produce more zonally symmetric structures, with exception of UKMO, GFDL and CSIRO models. Almost all models capture the explained variance of this mode, but MIROC fails in reproducing the explained variance of this mode (overestimates the explained variance by more than 10%). The second and third EOFs, referred to as the PSA1 and PSA2 patterns, respectively (Mo and Higgins 1998), emerge as the leading circulation patterns in the SH, based on hemispheric or sectorial analyses, ranging from daily (Mo and Ghil 1987), intraseasonal (Mo and Higgins 1998, Ghil and Mo 1991), interannual (Kidson 1988, 1999) to interdecadal timescales (Garreaud and Battisti 1999). PSA1 mode is characterized by centers of anomalies extending from the tropical eastern Pacific towards southern South America, representing the atmospheric response to ENSO forcing. All models reproduce well the spatial structure of the PSA1 mode, though they systematically underestimate the associated
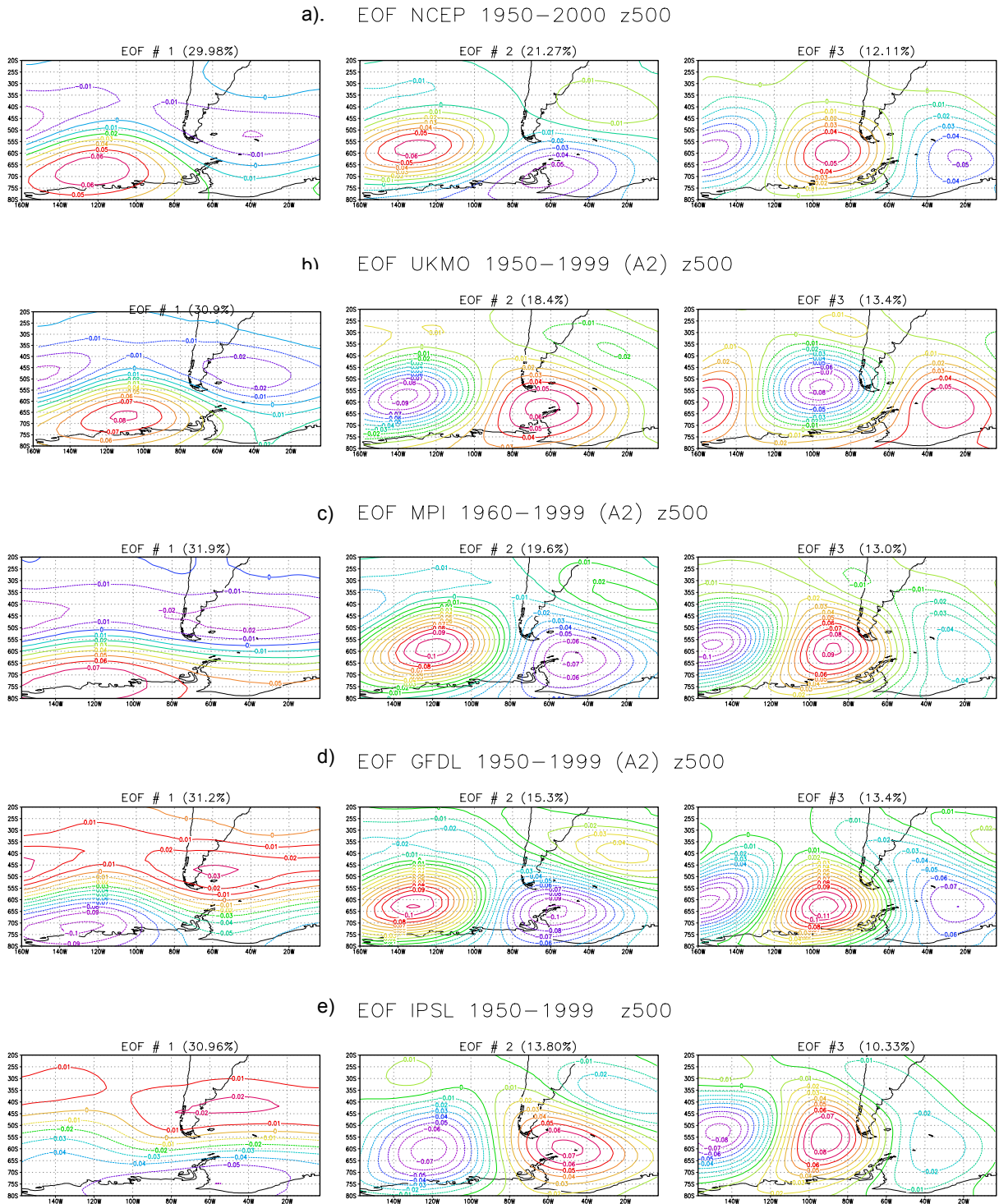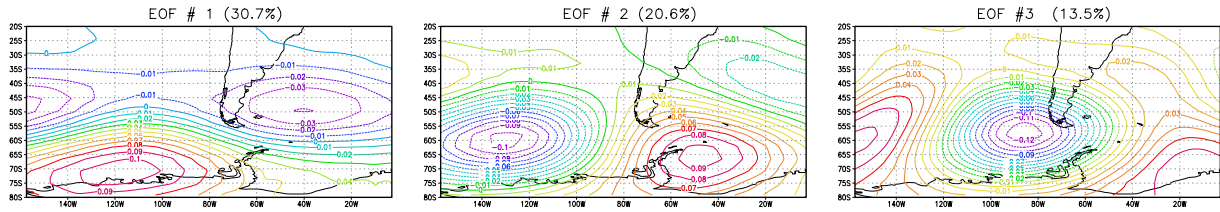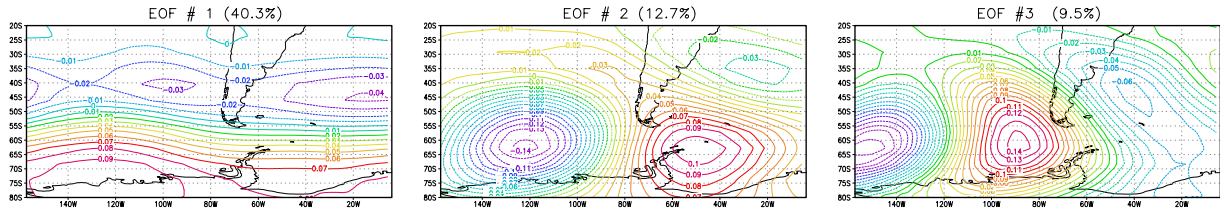
Figure 1: First three leading EOFs of the detrended monthly mean 500 hPa geopotential height calculated for the 50-year corresponding to present climate (1950-2000) derived from a) NCEP reanalysis; b) UKMO ; c) MPI, d) GFDL and e)IPSL AOGCMs . The variance explained by each EOF in percentage is listed on the top of each anel. Dashed contours represent negative values.
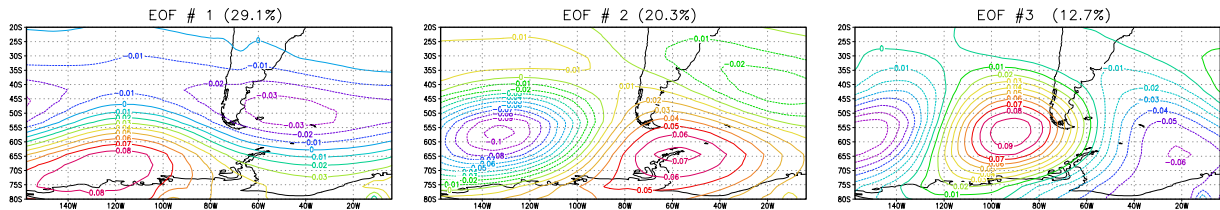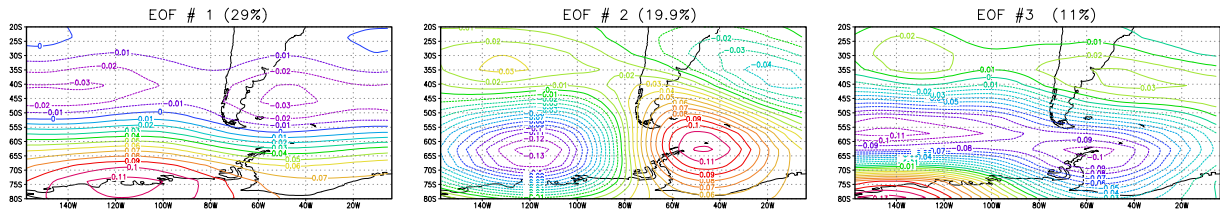
Figure 1 (cont.): f) NCAR; g) MIROC; h) CSIRO and i) CNRM.

explained variance, being the MIROC, the IPSL and the GFDL, the models that more strongly underestimate this variance. This common behavior may be associated with too weak ENSO-like sea surface temperature anomalies in all models. The standard deviation of the time series corresponding to each mode (see Table 2) are systematically underestimated by all models, being the IPSL model in better agreement with NCEP and the CNRM model showing larger discrepancies (the standard deviation of the time series corresponding to each mode are less than 40 % of the observed). The underestimation of the variability associated to each mode suggests that for all models interannual and interdecadal variability are weaker than in observations. This is a common feature of AOGCMs (Zwiers and Kharin, 1998). Nevertheless, this new generation of AOGCMs seems to evidence a better agreement with NCEP reanalysis compared with previous versions of these models (Solman and Le Treut, 2006; CMIP2 report at http://www-pcmdi.llnl.gov). The third mode, the so called PSA2, is well represented in terms of its spatial characteristics and explained variance by almost all models. Exceptions are the CNRM model which ranks this mode as the fourth mode with less explained variance than in NCEP reanalysis, NCAR model which shows marked differences in the spatial pattern and MIROC which fails in reproducing both the explained variance and the spatial structure of this mode.

Overall, while some deficiencies in reproducing some characteristics of the low-frequency variability patterns, all the models are able to reproduce reasonably well the main characteristics of patterns of low-frequency variability over the region.

The way in which the anomalies have been defined in this study allows evaluating climate change as a change in the mean conditions superimposed to a change in the variability. Before analysing whether the physical structure of the patterns of natural variability remain stationary or not, we will first analyze to what extent the 20th century simulated trend agree with observations.

444

For present climate conditions, trends in 500 hPa geopotential height field have been approximated as the best linear regression. The linear trend field for the period 1950-1999 (not shown) in NCEP reanalysis presents a spatial structure similar to the positive phase of the AAO-pattern, with negative values at high latitudes, with a minimum of -100 m/50 yrs to the west of the Antarctic Peninsula (130°W) and positive values at mid-latitudes and subtropical latitudes, with a maximum of 50 m/50 yrs over the southern tip of South America. In other words, the well documented positive trend towards the positive phase of the AAO in recent decades (Marshall, 2003). This trend has been attributed to several forcings, such as ozone depletion (Thomspon and Solomon, 2002); increasing greenhouse gases concentration (Kushner et al., 2001) and natural forcings as well (Hartmann et al., 2000). The structure of the linear trend for the present-day climate conditions as depicted by the AOGCMs is qualitatively and quantitatively different from the observations. All models underestimate the magnitude of the trend and fail in reproducing its spatial structure. Moreover, in many models the spatial structure of the trend does not project onto the first EOF, as observed. Only the CNRM, UKMO and NCAR models agree better with observations in terms of the spatial structure of the trend, but the magnitude is 40% weaker. The discrepancy between the observed and simulated strength and structure of the trend merits further research to understand the causes of this misrepresentation. It is important to remark that the models should include all the observed forcings and should also capture the internal interdecadal variability in order to represent the trend adequately. Nevertheless, these research issues are beyond the scope of the present study.

In order to address the stability of the main modes of variability under increased external forcing, we performed the EOF analysis for the entire dataset, corresponding to the period from 1950 to 2099, and for two sub-samples representing present (1950-2000) and future climate conditions (2050-2099), respectively. The ranking and the spatial characteristics of the three leading EOFs for both periods and for the period spanning the 150 years, remain unaltered. Moreover, the corresponding Principal Components (not shown) do not present any trend, which suggests that the low-frequency variability in the transient simulations analysed do not present any significant response in terms of patterns to altered mean conditions. Table 1 show the explained variance of each EOF for different sub-samples. The standard deviation of the times-series of each mode for each period analysed are displayed in Table 2. For almost all models the percentage of explained variance of each mode for both periods corresponding to present climate and SRESA2 scenario, do not show any significant change. UKMO and IPSL present larger differences in the percentage of explained variance, being larger for SRESA2 scenario than for present conditions. Nevertheless, the standard deviations of the corresponding time-series of each mode for all models do not differ significantly for both periods

analysed. In summary, the differences in explained variances found between both periods are subtle and it can be concluded that these main modes of low-frequency natural variability still remain unaltered under a transient increase of external forcing, suggesting they depend more on the internal dynamics of the atmospheric flow than on its external forcing. This result agrees with previous findings (Solman and Le Treut, 2006) and confirms one of the hypothesis drawn by Palmer (1999) concerning that the physical structure of the patterns of natural variability remain unaltered.

Once the stability of the main modes of variability has been verified, it is possible to perform the cluster analysis to identify the recurrent patterns for the entire dataset. This will allow us to identify the changes in the regime population throughout the total period analysed. The cluster analysis was performed on the 150 years of monthly anomalies for the eight models analysed with a prescribed number of clusters from 2 to 8. The number of regimes constituting the most significant partition for each model varies from 3 to 6 regimes. For some of the models no significant partition for the entire dataset was found, so we decided to force de classification to the number of clusters which classifiability index was nearest the upper bound of significance.

Overall, Regime 1 and Regime 2 resemble different phases of the Antarctic oscillation-like pattern of variability (the positive/negative phase of the AAO has lower/higher geopotential height anomalies over the polar regions), and correspondingly, they compare mainly with EOF 1 pattern, though slightly modulated by the contribution of EOFs 2 and 3. Regime 1 resembles the spatial structure of the positive phase of AAO-mode and Regime 2 resembles the spatial structure of the negative phase. Regimes 3, 4, 5 and 6 exhibit a PSA-like pattern, corresponding to different phases of a westward propagating wave-train. Regimes 3 and 4 differ primarily in sign, corresponding to positive and negative phases of EOF 2 pattern, respectively, corresponding to a positive/negative anomaly eastern the Antarctic Peninsula, respectively. Regime 5 matches with the positive phase of the EOF 3 pattern, corresponding to a positive anomaly western the Antarctic Peninsula. Regime 6 represents a combination of EOFs 2 and 3.

Table 3 shows the frequency of occurrence of each regime for each model for the entire period. The frequency of occurrence is defined as the total number of months falling into each regime divided by the total number of months classified. For all models Regime 1 and Regime 2 appear as frequented regimes, being Regime 1, corresponding to the positive phase of the AAO-like pattern, more frequented than Regime 2. Both phases of the PSA1-like mode, say, Regimes 3 and 4 represent recurrent patterns, though for some models only one of them appear as a recurrent pattern in the classification. Regimes 5 and Regime 6 appear as recurrent regimes only for two models.

	EOF	NCEP	UKMO	MPI	GFDL	IPSL	NCAR	MIROC	CSIRO	CNRM
20c3m 1	1	30.0%	30.9%	31.9%	31.2%	31.0%	30.7%	40.3%	29.1%	29.0%
	2	21.3%	18.4%	19.6%	15.3%	13.8%	20.6%	12.7%	20.3%	19.9%
	3	12.1%	13.4%	13.0%	13.4%	10.3%	13.5%	9.5%	12.7%	11.0%
sresa2	1		37.0%	33.9%	34.9%	36.3%	33.9%	36.1%	34.3%	30.8%
	2		17.5%	18.1%	16.0%	16.4%	18.4%	13.6%	17.1%	22.6%
	3		13.6%	12.9%	11.3%	11.3%	14.0%	11.7%	13.2%	10.3%
total	1		36.6%	36.6%	33.1%	34.0%	34.5%	35.9%	32.2%	28.9%
	2		17.4%	18.5%	15.3%	14.6%	18.9%	14.3%	18.5%	20.6%
	3		14.0%	13.1%	12.1%	10.9%	13.9%	10.8%	12.7%	11.3%

Table 1: Percentage of explained variance for the first three EOFs for different sub-samples for each model.

	EOF	NCEP	UKMO	MPI	GFDL	IPSL	NCAR	MIROC	CSIRO	CNRM
20c3m	1	1041.7	832.8	833.17	633.63	982.8	650.4	524.68	570.3	388.63
	2	877.4	642.9	653.79	444.21	656.07	533.38	294.48	476.24	322.52
	3	662.1	548.3	532.65	416	567.76	430.97	254.55	377.75	239.13
sresa2	1		961.52	847.7	670.35	1076.07	664.93	483.63	623.23	397.33
	2		662.14	619.91	453.65	723.29	490.59	297.27	438.71	339.99
	3		582.52	523.81	380.98	599.51	427.97	275.75	386.01	229.55
total	1		868.86	835.66	670.35	1032.19	1064.46	943	606.46	748.63
	2		634.91	629.86	453.65	675.45	788.46	594.98	459.07	631.58
	3		568.39	529.48	380.98	584.1	675.4	516.01	380.68	467.87

Table 2: The standard deviation of the time series corresponding to the first three sectorial EOFs derived from different models for different sub-samples.

Table 3: Percentage of months belonging to each regime (regime frequency) for each model (top) and change in

		Regime	UKMO	MPI	GFDL	IPSL	NCAR	MIROC	CSIRO	CNRM
Regime frequency	**1950-2099**	1	37.5%	19.10%	47.10%	17.90%	29.60%	30.50%	42.30%	39.80%
		2	21.8%	9.70%	27.30%	12.30%	15.00%	16.40%	29.20%	33.70%
		3	40.9%	20.30%		20.50%	32.50%	28.30%		
		4		15.70%	24.90%	19.60%	23%	24.70%	28.50%	26.40%
		5		19.40%		14.50%				
		6		15.70%		15.30%				
Regime population change (%)	**(2050-2099)-(1950-1999)**	1	1.7	1.5	1.7	1.3	-3.8	-4	1.8	0.2
		2	1.0	0	0.5	1	-0.7	-0.8	-3.7	-1.2
		3	-2.7	-3.4		-1.7	3.4	2		
		4		1.6	-2.2	-1.2	1	2.8	1.8	1
		5		-0.6		-1.3				
		6		0.9		1.8				

regime population (as a percentage) of each regime for the period 2050-2100 relative to 1950-2000.

In order to test whether climate change can be interpreted in terms of a change regime population, we compare the population of each regime for the first fifty years of the period analysed, say present conditions (1950-1999), with those found for the last fifty years (from 2050 to 2099). The mean population of each regime for each fifty-year period is defined as the total number of months falling into each regime divided by the number of years, thus, giving a measure of the mean annual distribution of regimes throughout the corresponding period. Results of the change in population are given in Table 3. A student t-test has been applied to assess the significance of the changes, as in Hsu and Zwiers 2001. For all the models, no significant changes in the population of any of the regimes have been found. This result suggests that, in terms of the low-frequency variability behaviour, climate

change does not alter the spatial and temporal characteristics of the leading modes of internal variability neither manifest itself as a change in regime population.

The result found in this study differs from a previous study in which the IPSL- CCM2 AOGCM was evaluated (Solman and Le Treut, 2006). In the case of IPSL-CCM2 AOGCM it was shown that, under enhanced greenhouse gas forcing, a significant change in frequency of occurrence of several regimes was found. In that case, the negative phase of the AAO-like pattern became more frequented at the expense of the positive phase. Thus, climate change was manifested as a strong trend superimposed to a change in the frequency of occurrence of the more frequented circulation patterns. Moreover, the change in regime frequencies reflected the evidence that the circulation patterns of low-frequency variability (interannual to interdecadal) changed in opposite phase with respect to the mean climate, so these patterns of variability superimposed to a changing mean state modulate the climate change signal. The results found in the present work, however, do not invalidate previous findings, as the AOGCMs are continuously being improved and their response under anthropogenic forcing, particularly concerning to atmospheric variability, is a research topic that merits further development.

Finally, after having demonstrated that climate change does not manifest as a change in low-frequency variability patterns, we analyse the climate change signal. Though we have also shown that the AOGCMs do not reproduce adequately observed trends, which are a response to several forcings, the climate change signal in the SRESA2 simulations represent the response to anthropogenic forcing only. Thus, the question to be addressed is whether the climate change signal can be projected onto patterns corresponding to main leading modes of variability. Several previous studies (Stone et al. 2001; Fyfe et al. 1999, Carril et al., 2005) based on hemispheric analysis, have shown that in the Southern Hemisphere the climate change signal projects mainly onto the AAO-like pattern.

The climate change signal has been calculated as a linear trend throughout the period from 1950 to 2099. Figure 2 shows the spatial pattern of the trend as depicted by the 8 AOGCMs analysed. The spatial pattern of the climate change signal shows an increase of the north-south gradient as consequence of a major increase of the 500 hPa geopotential height over mid-latitudes and a weaker increase over high latitudes. Major increases over subtropical latitudes, ranging from 60 to 120 meters, depending on the model, are found over the Atlantic and Pacific Oceans. The minimum increase is found, for almost all models, western the Antarctic Peninsula. All the models agree in that the spatial pattern of the trend at 500 hPa resembles the spatial structure of the respective AAO-mode, in agreement with previous studies.. This behaviour suggests a trend towards the positive phase of the AAO pattern.

In summary, low-frequency variability, in terms of the leading modes of variability and circulation regimes, remain unaltered under anthropogenic forcing. Climate change manifests as a trend, towards the positive phase of an AAO-like pattern, which is superimposed to stationary internal low-frequency variability patterns. This result agree with those found by Fyfe et al. 1999, who showed that the modelled AAO behaviour remains unchanged but rather superimposed on the forced climate change, in his analysis of a transient climate change simulation.

4. SUMMARY AND CLONCLUSIONS

In this study we have focused on the low-frequency variability of the southern South America circulation and its response to greenhouse gas forcing. Last generation 20th and 21st century simulations performed with a set of 8 Atmosphere - Ocean General Circulation Models (AOGCMs) participating in the IPCC Fourth Assessment Report (AR4) were analyzed. Our main goals were, first, to evaluate the capability of the models to represent observed low-frequency variability and trends. Then, to explore the behaviour of the leading modes of low-frequency variability, from interannual to interdecadal scales, in order to evaluate whether they remain invariant in a forced scenario. We also explored the behaviour of the circulation regimes that characterise the regional circulation, in order to evaluate whether climate change can be interpreted as a change in population of the more recurrent circulation regimes. Finally, we analysed the structure of the climate change signal.

All calculations are based on monthly mean 500 hPa heights. Anomalies are defined with respect to a 11-year running mean throughout the period 1950-2099.

Overall, the AOGCMs analyzed are able to capture the broad spatial structure of the main sectorial modes of observed low-frequency variability, say the Antarctic Oscillation mode (AAO) ranging as the first leading mode, and the Pacific South America modes (PSA1 and PSA2) ranging second and third, respectively, though some features appear misplaced, compared with NCEP reanalysis. Nevertheless, all the models systematically underestimate the explained variance associated to the PSA1 pattern, characterized by centers of anomalies extending from the tropical eastern Pacific towards southern South America, representing the atmospheric response to ENSO forcing. This common behavior may be associated with too weak ENSO-like sea surface temperature anomalies in all models. The linear trend for the present-day climate conditions was compared against NCEP and it was found that only few models are capable to represent adequately the last 50 years observed trend. All models underestimate the magnitude of the trend and fail in reproducing its spatial structure. Moreover, in many models the spatial structure of the trend does not project onto the first EOF, as observed. Only the CNRM, UKMO and NCAR models agree better with observations in
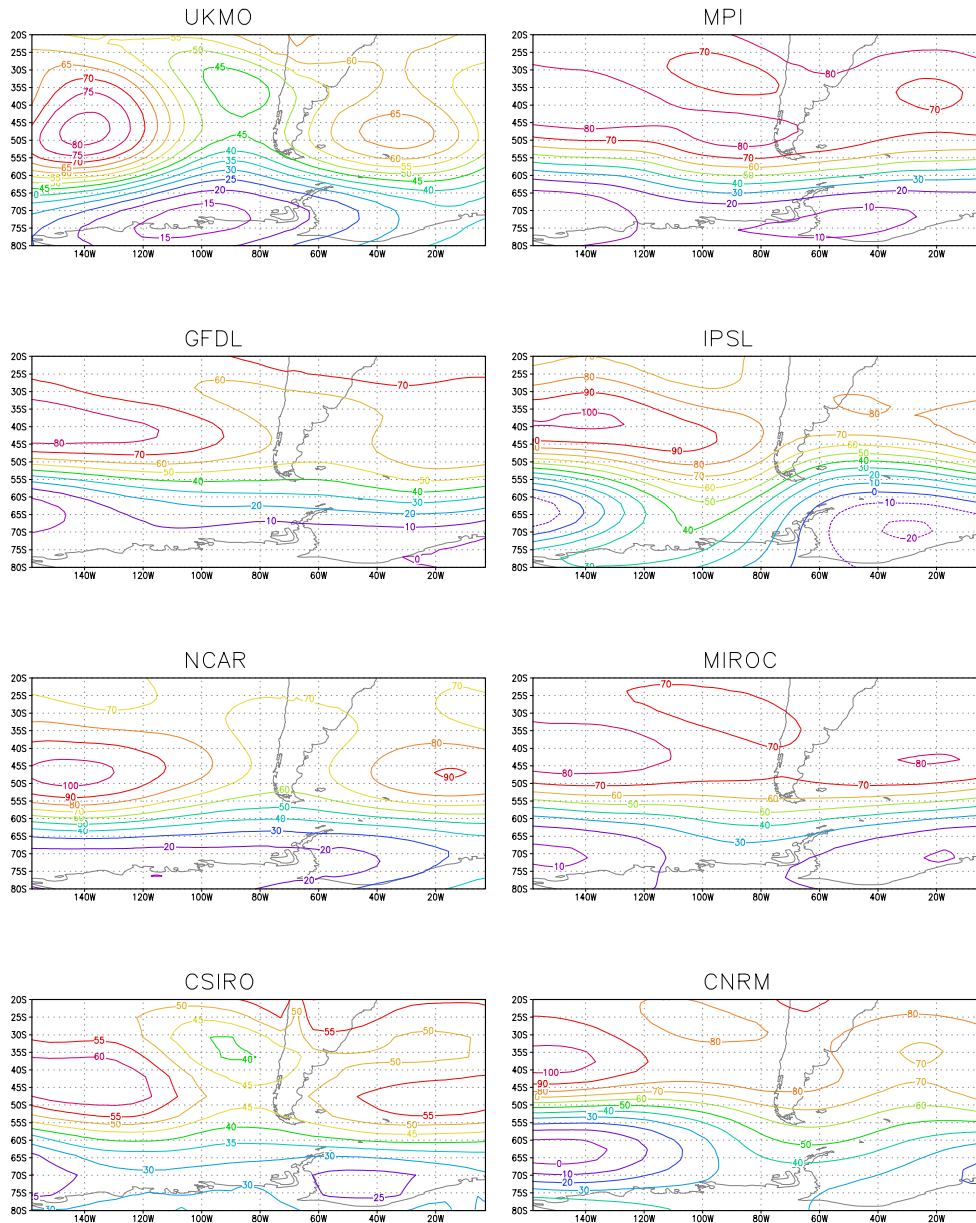
Figure 2; Linear trend of the 500 hPa monthly mean field for the period 1950-2099 from the 8 AOGCMs analysed.

terms of the spatial structure of the trend, but the magnitude is 40% weaker.

The stability of the main patterns of variability was then explored by performing an EOF analysis for different periods: 1950-1999, 2050-2099 and 1950-2099. We found that in all models the main modes of low-frequency variability remain unaltered under a transient increase of external forcing, in terms of both, their spatial temporal characteristics, suggesting they depend more on the internal dynamics of the atmospheric flow than on its external forcing.

Inspection of the circulation regimes derived for the period 1950-2099 for all models showed no significant change in population of any regime. Moreover, climate change manifests as a positive trend with a pronounced increase of the 500 hPa heights at subtropical latitudes and a weaker increase over high-latitudes. The spatial structure of the trend resembles the spatial pattern of the AAO-mode, in all models, in agreement with previous findings. In summary, low-frequency variability, in terms of the leading modes of variability and circulation regimes remain unaltered under anthropogenic forcing. Climate change manifests as

a trend, towards the positive phase of an AAO-like pattern, which is superimposed to stationary internal low-frequency variability patterns.

References

Carril A., Menéndez C., Navarra A. , 2005: Climate response associated with the Southern Annual Mode in the surroundings of Antarctic Peninsula: a multi-moel ensemble analysis. *Geophys. Res. Lett.*, 32, doi:10.1029/2005GL023581.

Fyfe J., Boer G., Flato G. , 1999: The Arctic and Antarctic Oscillations and their Projected Changes under Global Warming. Geophys Res Lett 26: 1601-1604.

Garreaud RD, Battisti DS, 1999: Interannual (ENSO) and interdecadal (ENSO-like) variability in the Southern Hemisphere tropospheric circulation. J Climate 12: 2113 – 2123.

Ghil M, Mo K .,1991: Intraseasonal oscillations in the global Atmosphere. Part II: Southern Hemisphere. J Atmos Sci 48: 780-790.

Hartmann, DL., JM Wallace, V. Limpasuvan, DW. Thompson and JR. Holton, 2000: Can ozone depletion and global warming interact to produce rapid climate change? *Proceedings of the National Academy of Sciences of the USA*, 97, 1412-1417.

Hsu CJ, Zwiers F., 2001: Climate change in recurrent regimes and modes of Northern Hemisphere atmospheric variability. J Geophys Res 106: 20145-20159.

Kageyama M, D´Andrea F, Ramstein G, Valdes PJ ., 1999: Weather regimes in past climate atmospheric general circulation model simulations. Clim Dyn 15: 773-793.

Kidson JW., 1988: Interannual variations in the Southern Hemisphere circulation. *J Climate* 1: 1177-1198.

Kidson JW., 1999: Principal modes of Southern Hemisphere low frequency variability obtained from NCEP/NCAR reanalyses. *J Climate* 12: 2808-2830

Kushner, P.J., I. Held and T. Delworth, 2001: Southern Hemisphere Atmospheric Circulation Response to Global Warming. J. Climate, 14, 2238-2249.

Marshall. G.J., 2003: Trends in the Southern Annular Mode from observations and reanalysis. J. Climate, 16, 4134-4143.

Michelangeli PA, Vautard R, Legras B., 1995): Weather regimes: Recurrence and quasi stationarity. J Atmos Sci 52: 1237-1256.

Mo K, Higgings RW., 1998: The Pacific-South American modes and Tropical Convection during the Southern Hemisphere winter. Mon Wea Rev 126: 1581-1596.

Mo K, Ghil M., 1987: Statistics and dynamics of persistent anomalies. J Atmos Sci 44 : 877-901.

Palmer T., 1999: A nonlinear dynamical perspective on climate prediction. J Climate 12: 575-591.

Solman S. And H. and Le Treut (2006): Climate change in terms of modes of atmospheric variability and circulation regimes over southern South America. Clim. Dyn., in press.

Stone D, Weaver A, Stouffer R.,2001: Projection of Climate Change onto modes of Atmospheric Variability, .J Climate 14: 3551-3565.

Thomspon D. W. and S. Solomon, 2002: Interpretation of recent Southern Hemisphere climate change. Science, 296, 895-899.

Yang S, Reinhold B., 1991: How does the low-frequency variance vary? Mon Wea Rev 119: 119-127.

Zwiers FW, Kharin VV., 1998: Intercomparison of interannual variability and potential predictability: An AMIP diagnostic sub-project. Clim Dyn 14: 517-528.